Section 3

Computational studies including new techniques, parallel processing, GPUs. Effects of model resolution.

Systematic errors due to terrain-following coordinates

Fedor Mesinger (1) and Katarina Veljovic (2)

(1) Serbian Academy of Sciences and Arts, Belgrade, Serbia (fedor.mesinger@gmail.com)
(2) Inst. of Meteorology, Faculty of Physics, Univ. of Belgrade, Serbia (katarina@ff.bg.ac.rs)

Over past decades, various sets of tests have been done comparing the results of the Eta against its version switched to sigma. In all of them the eta version did better. However, a poor result of an Eta in case of a windstorm, and an experiment of Gallus and Klemp, led many to consider the eta to be "ill suited for high-resolution models." Still, in a 5+ month parallel test the Eta/EDAS system had better precipitation scores than the WRF-NMM/GSI put together to replace it (Mesinger and Veljovic 2017, Fig. 4). Following a refinement of the eta discretization making it a simple cut-cell scheme, the Gallus-Klemp separation of the flow behind a bell-shaped topography was shown not to occur (ibid., Fig. 7).

Tests of the impact of the use of the eta resumed via experiments with the Eta driven by ECMWF (EC) 32-day ensemble members. Using a score verifying placement of strongest 250 hPa winds, chosen to be those of speeds > 45 m s^{-1}, as well as the rms wind difference, generally advantage of the Eta was seen in spite of about the same resolution of two models during the first 10 days of the experiment (ibid., Section 5). This advantage was particularly visible when a deep upper tropospheric trough was crossing the Rockies the first 2-6 days of the experiment. Here in Fig. 1 we show 250 hPa wind averages for all 21 members, at day 4.5; see figure legend for the content of its panels.

While predicting the major pattern, EC members do not extend the > 45 m s^{-1} jet streak entering Alaska sufficiently southeastward, and have the streak across contiguous U.S. too

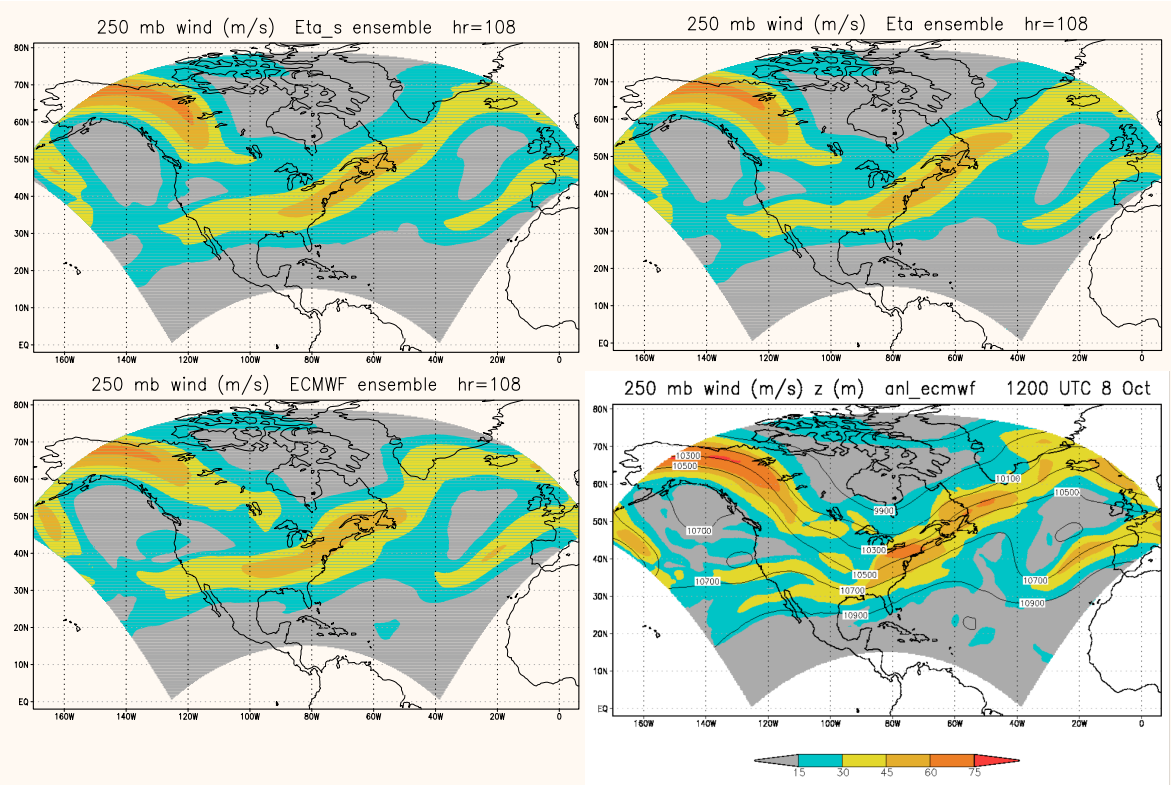

Fig. 1. Ensemble average, 21 members, at 4.5 day time: EC verification analysis bottom right, EC driver members bottom left, Eta members top right, Eta/sigma members top left.

far westward. These features are improved on Eta maps, in particular by the Eta/eta in terms of covering a bit of the eastern Labrador, and more of the ocean area towards the tip of Greenland and off the U.S. New England states.

The advantage of the Eta is demonstrated to even a greater degree by the number of "wins" of one model vs. another. Thus, in Fig. 2, left panel, number of wins of the Eta winds > 45 m s^{-1} and its EC driver members vs. each other are shown as a function of time, according to the score that verifies the accuracy of the *placement* of the variable verified, Equitable Threat (or Gilbert) Score, adjusted to unit bias, ETSa. Same, but according to the RMS difference of forecast and analyzed winds, right panel.

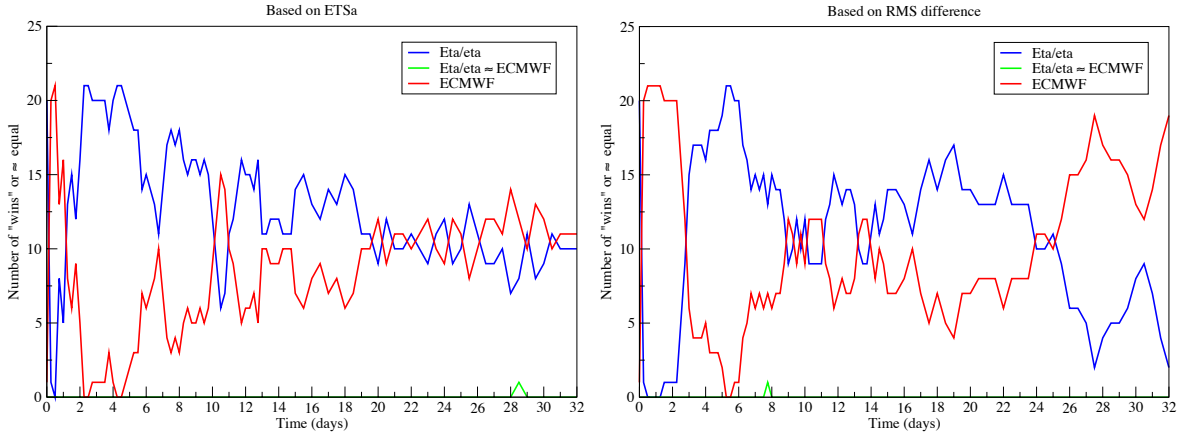

Fig. 2. Number of "wins" of one model vs. another: blue, Eta/eta, red, their EC driver members.

Initially the EC members have an advantage presumably due to errors the Eta members absorb due to initializations off their EC members. The advantage of the Eta later on is particularly striking in the ETSa scores of days 2 to 6, with 4 verifications in which all 21 Eta members have better strongest winds placement scores than their EC driver members.

An important issue is what features of the Eta are the leading contributors to its performance seen in Fig. 2? One on which we have information is again the impact of the eta vs. sigma coordinate, Fig. 3. While the Eta/sigma is still clearly "winning," it does not win with such a total advantage of winning repeatedly all the 21 members.

We are somewhat puzzled by the Eta/sigma performance shown being not that much inferior to that of the Eta/eta. In the Eta/eta vs. Eta/sigma plot, not shown, overwhelming advantage of the Eta/eta is however seen in the early period, with 7 wins for all the 21 Eta/eta members. Reasons possibly helping the Eta/sigma display such a perhaps unexpected advantage over the EC as seen in Fig. 3 are discussed in our reference.

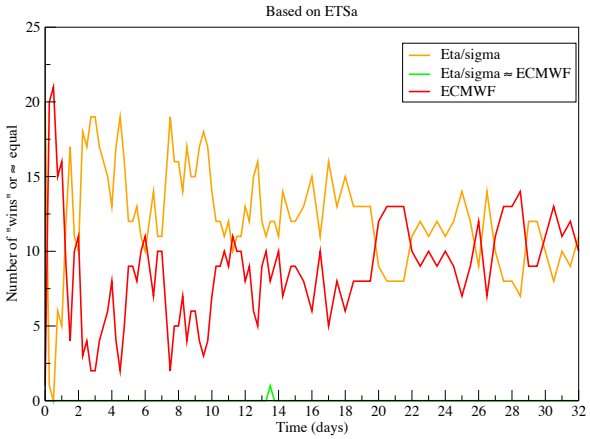

Fig. 3. As Fig. 2, left panel, but for the Eta/sigma (orange) vs. its EC driver members.

Reference:

Mesinger F., and Veljovic K., 2017: Eta vs. sigma: Review of past results, Gallus-Klemp test, and large-scale wind skill in ensemble experiments. *Meteorol. Atmos. Phys.*, doi:10.1007/s00703-016-0496-3

Conformal localized-overset polyhedral global grids based on Riemann surfaces

R. James Purser
IMSG at NOAA/NCEP/EMC, College Park, MD 20740-3818, U.S.A. (Email: jim.purser@noaa.gov)

1. Introduction

The age of massively-parallel computing brought about a resurgence of interest in using polyhedral grids, especially the cube and the icosahedron, as the computational horizontal frameworks of global atmospheric models (Ronchi et al., 1996; McGregor 1996; Rančić et al., 1996). Such grids are quasi-uniform and, unlike the latitude-longitude framework, do not suffer communications burden of operators (such as the Fourier filters) needing an immediate global reach.

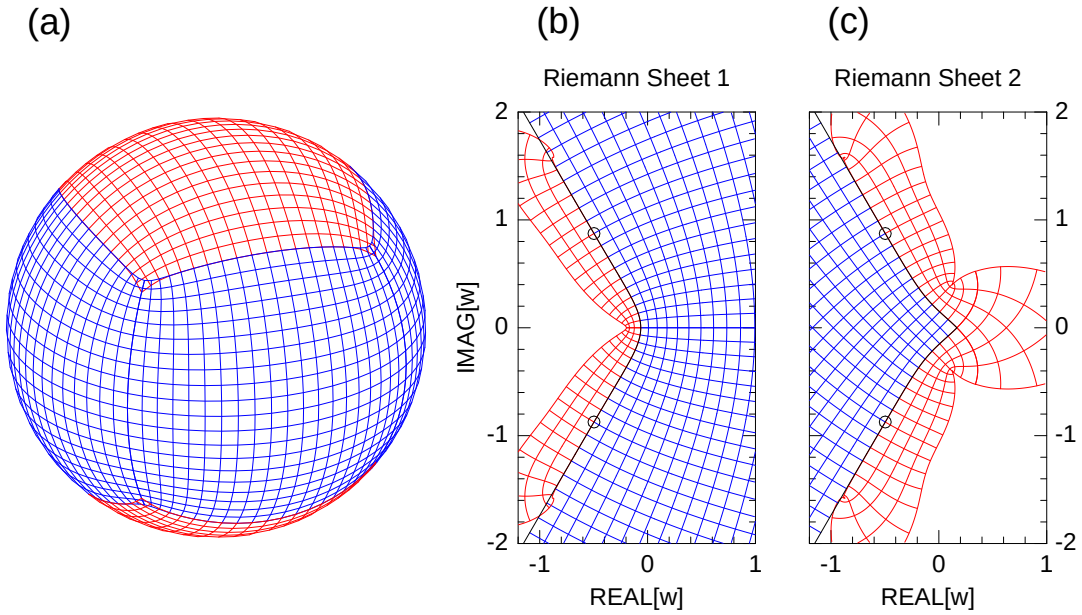

Figure 1. (a) A conformal cubed-sphere grid with Riemann surface corner oversets. (b) and (c) show two sheets of the associated idealized planar Riemann surface.

But a polyhedron has edges and corners, which poses other numerical difficulties. Rančić et al. (1996) and Purser and Rančić (1998) eliminated the edge discontinuities by adopting conformal mapping schemes, but intense grid curvature and unbounded resolution is a consequence of these mappings around the singularities that remain – the corners. This renders these otherwise attractive grid geometries disadvantageous in their original forms.

In order to achieve the considerable benefits of having exactly conformal grids, but without the problems associated with strong corner singularities, it is possible to "overset" separate conformal grids whose singularities are banished to distant regions of each tile, beyond the highly regular regions of active numerical interest where curvature and resolution excursions remain small. One way to do this is by using two conformal Mercator grid overset in the so-called "Yin-Yang" configuration (Kageyama and Sato 2004). But we still pay the price of

having to carry out reconciling interpolations and blending around the entire globe-girdling zone of overlap.

An attractive variant suggested by the methods of complex analytic function theory by which conformal mappings are generated, is to exploit the feature of "Riemann surfaces" that are associated with mappings in which the domain of the function comprises two "sheets" sharing the same complex coordinate. The overset region is kept to small geographical areas, as shown in panel (a) of the figure, bounded by a pair of branch point singularities located a short distance away from the overlapping tile's corner, one on each edge. The mapping function near either one of these singularities can be expanded in powers of the complex coordinate relative to the singularity using half integer powers, which causes the inverse mapping to have the two-valuedness associate with the self-overlapping Riemann surface. But the first few half-odd-integer powers can be suppressed in the construction by allowing extra compensatingly singular degrees of freedom to occur in the expanion of the function "about infinity" in the sheet corresponding to the noncomputational portion of the solution (shown as the red portions of the idealized corner detail of panels (b) and (c) of the figure).

The method of construction involves a generalization to the Riemann surface topology of the "Schwarzian" iteration, used in Rančić et al. (1996), in which each piece of the solution is described by a convergent power expansion about a nearby point, and all points along the circle of convergence of a given expansion lie well within at least one disk of convergence of another of the power expansions. Complex Fourier transformation of the diagnosed interim solution along a circle (or a circuit conformally-equivalent to a circle) just within the convergence limit enables refinement of the associated expansion coefficients, and a sequence of iterations from an initial crude guess-solution, leads towards the desired analytic solution. The only singularities – the branch points – should remain sufficiently weak to be essentially invisibe to numerics of a dynamical model core, whether it be of the finite difference or the finite volume kind. By careful reconciliation of the duplicated solutions in the small overlap regions, it is expected that grid-imprinting effects, even in extended period model runs, could be rendered insignificant.

References

Kageyama, A., and T. Sato 2004 The "Yin-Yang grid": An overset grid in spherical coordinates. *Geochem., Geophys. Geosyst.,* **5,** Q09005, *doi: 10.1029/2004GC000734.arXiv.org:physics/0403123*

McGregor, J. L. 1996 Semi-Lagrangian advection on conformal-cubic grids. *Mon. Wea. Rev.,* **124,** 1311–1322.

Purser, R. J., and Rančić, M. 1998 Smooth quasi-homogeneous gridding of the sphere. *Quart. J. Roy. Meteor. Soc.,* **124,** 637–647.

Rančić, M., R. J. Purser, and F. Mesinger 1996 A global shallow-water model using an expanded spherical cube: Gnomonic versus conformal coordinates. *Quart. J. Roy. Meteor. Soc.,* **122,** 959–982.

Ronchi, C., Iacono, R. and Paolucci, P. S. 1996 The 'cubed sphere': A new method for the solution of partial differential equations in spherical geometry. *J. Comput. Phys.,* **124,** 93–114.